Monitoring the electrical properties of metal ore mine tailings during sedimentation

Monitoring the electrical properties of metal ore mine tailings during sedimentation

R. Monroy[1*]

W. J. McCarter[2]

[1] Eur Ing, BEng, MSc, DIC, PhD, CEng, MICE

Amec Foster Wheeler

Canada Square, Canary Wharf, London, E14 5LQ, United Kingdom

rafael.monroy@amecfw.com

Tel.: +44 207 532 0165

[2] BSc, PhD, DSc, CEng, MICE

Heriot Watt University,

School of Energy, Geoscience, Infrastructure and Society, Edinburgh, EH14 4AS, United Kingdom

w.j.mccarter@hw.ac.uk

* Corresponding Author

Date of preparation of current version: 14/07/2017

Word count: 3160

Figures: 12

ABSTRACT

Material characterisation and process monitoring in particulate media can be enhanced by measuring electric properties. In this study, the temporal changes in electrical resistivity were recorded during the sedimentation of gold and copper mine tailings (i.e. crushed rock particles deposited as a slurry). A small sedimentation column, fitted with four sets of electrodes, was used to perform undrained settling tests on slurries with solids contents over the range 50%-65%. It was observed that during sedimentation, the electrical resistivity increased to a constant steady-state value as the porosity of the slurry decreased. The data was modelled using Archie's law to highlight the effect of pore-fluid resistivity, porosity and tortuosity on the bulk resistivity of the tailings mass.

KEYWORDS: Contaminated material, fabric/structure of soils, strength and testing of materials.

1 INTRODUCTION

European Directive 2006/21/EC of the European Parliament and of the Council of 15 March 2006 on the management of waste from extractive industries EC (2006) requires the characterisation of the waste to be deposited in a storage facility in order to guarantee physical and chemical stability in the short and long term. Part of this characterisation process includes assessment of the geotechnical behaviour of the waste. For materials deposited as a slurry an important component of this assessment process consists of predicting the sedimentation and consolidation behaviour following deposition (Azam 2014a, 2014b).

During sedimentation, the waste solids will settle and leave a clear interface between the top of the settling mass and the supernatant fluid. This process is usually simulated in the laboratory by means of simple "jar settling tests", normally conducted in hydrometer cylinders. Slurry is poured inside the cylinder and the position of the slurry-fluid interface monitored, in order to obtain an indication of settlement rate and a minimum settle density. The tests can be carried out with underdrainage to simulate the presence of a high-permeability drainage layer below the waste. In this case the test is referred as "drained settling test". Otherwise, the test is known as an "undrained settling test".

The measurement of the electrical properties of particulate media offers an elegant and simple way to characterise materials and monitoring physio-chemical processes (Wagner and Scheuermann 2017). The subject has been explored in detail by Santamarina et al (2001), including the underlying principles and laboratory experimental techniques. In many instances, it is relatively simple to modify existing equipment to allow the electrical properties of geo-materials to be recorded whilst a test is conducted in the standard way.

This paper presents results from a laboratory-based study on the sedimentation of mine tailings (i.e. crushed rock particles deposited as a slurry) using a modified sedimentation column to perform undrained settling tests. Although results from electrical measurements recorded during sedimentation of soft sediments have been published (see, for example, Blewett et al 2001; Klein & Santamarina 2005), the Authors are not aware of similar tests carried out on mine waste derived from the

extraction of mineral products. Given the considerable volume of mine tailings produced every year, the environmental issues associated with their handling and storage, and the requirement to properly characterise their geotechnical properties, it is difficult to deny the benefits of exploring simple measuring techniques to study settling processes that could be developed for use both in the laboratory and in the field.

2 EXPERIMENTAL PROCEDURE

2.1 Material properties

Gold and copper tailings were used in the current study. The Authors had access to a limited sample, which had previously been de-toxified for geotechnical laboratory work. The original material contained a mixture of coarse and fine particles and, as the original intention was to test the finer fraction (also known as 'slimes'), material retained in the 0.3mm aperture sieve was discarded. The particle size distribution of the sample - obtained from a combination of wet sieving and sedimentation - is presented in Figure 1. The same figure also includes particle size distributions for fine and coarse gold and copper tailings taken from Blight (2010). It is evident that the particle size distribution of the selected material lies between the two sets of curves. Although not truly representative of fine tailings, it was decided to use this material in the study as further removal of coarser particles would have left to small a sample to perform the intended tests. The average specific gravity of the tailings, measured on a number of samples using a small pycnometer, was 2.88.

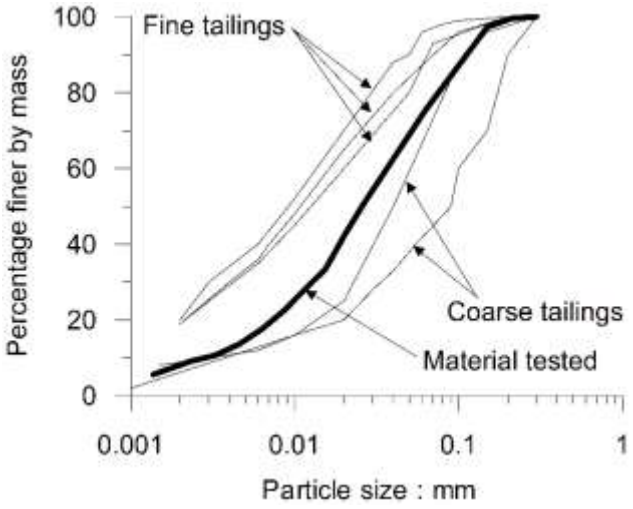

Figure 1. Particle size distribution of the tailings sample after removal of particles retained in the 0.3mm sieve. Also shown, curves for coarse and fine gold and copper tailings from Blight (2010).

2.2 Sedimentation column

The sedimentation column used in the study was a modification of that used by Blewett et al (2001, 2003) to study the sedimentation of a kaolin slurry and monitor ionic migration through consolidated kaolin. The acrylic column, shown in Figure 2, had internal dimensions of 50×50×519mm and included four sets of electrodes, with the mid-height of each set located at 35mm, 165mm, 295mm and 425mm above the base of the column. Each set of electrodes comprised a pair of 50×50mm stainless steel (s/s) plates placed flush with the sides of the column, together with a pair of small diameter (1.6mm) s/s rod electrodes. The rod electrodes were provided with heat-shrink sleeving to expose a 6mm tip; the electrodes themselves were separated by a horizontal distance of 20mm and protruded 12mm into the column.

The use of a four-terminal electrode arrangement, where the current electrodes (i.e. the s/s plates) and potential electrodes (i.e the s/s rods) are separated, eliminates measurement errors due to electrode polarization effects. As resistivity measurements are affected by temperature, a bead thermistor was mounted in a side wall of the sedimentation column. This allowed continuous monitoring of the slurry temperature, although tests were conducted in a temperature-controlled environment (20°C ± 2°C).

Electrical resistivity measurements were taken with an Agilent A4263B LCR meter set at a frequency of 1kHz with a signal amplitude of 100mV. Coaxial cables connected the measuring equipment to the electrodes; cable resistance was automatically nulled from the incoming data.

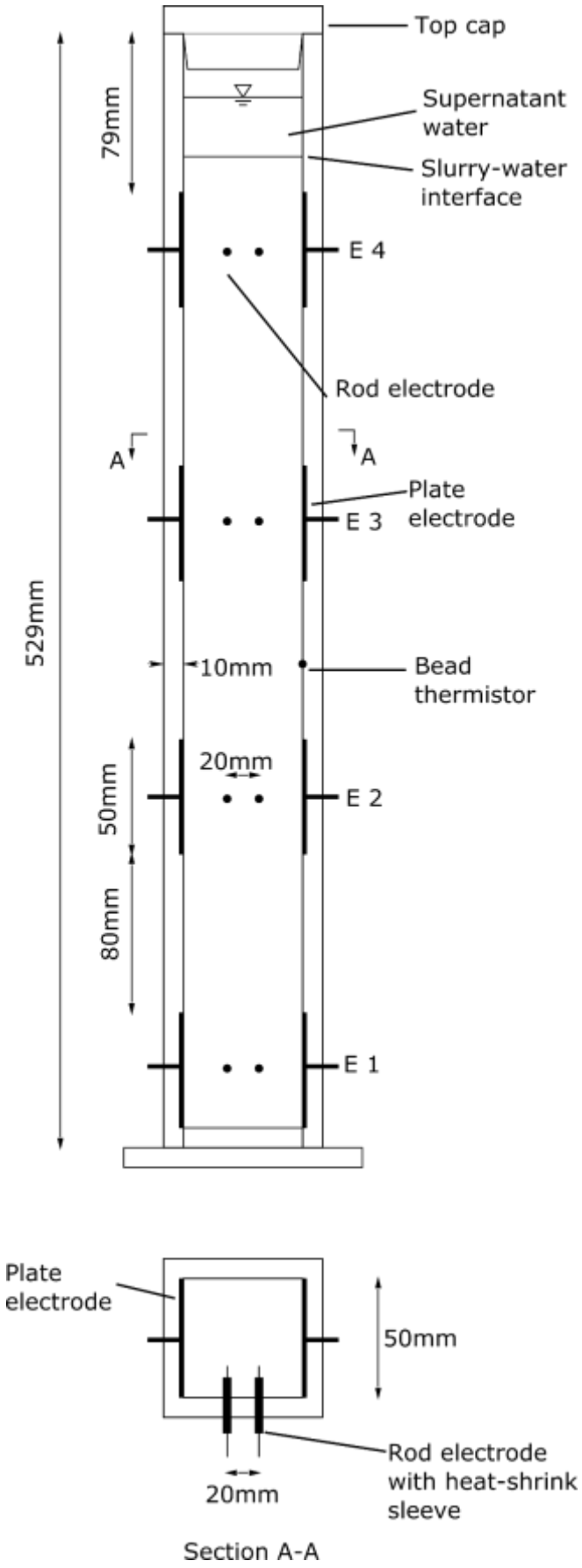

Figure 2. Sedimentation column showing location of electrodes (E1 to E4).

2.3 Calibration of the sedimentation column

The bulk resistivity of a prismatic sample of slurry (denoted ρ_{mix}, in ohm-m) placed between a pair of electrodes (i.e. parallel electrical field lines) can be obtained from the expression

$$\rho_{mix} = R\frac{A}{d} \quad (1)$$

where A is the electrode surface area (m^2), d is the electrode separation (m) and R is the bulk resistance of the mixture (ohm). In a four-terminal electrode arrangement, such as that shown in Figure 2, the electrode separation d corresponds to the distance between rod electrodes, which can be measured. However, fringing effects will result in a non-parallel electrical field distribution between the plate electrodes and hence an enlargement of the area occupied by the electrical field. It is not possible to measure the value of A directly and it becomes necessary to obtain the geometrical constant A/d experimentally for each set of electrodes through calibration with a liquid of known resistivity. This was achieved by filling the sedimentation column with different molarities (hence resistivity) of salt (NaCl) solution and measuring the resistance at each electrode position.

A small cuboidal cell, capable of containing a sample of volumetric dimensions 50×50×46mm and having an electrode arrangement similar to that used in the sedimentation column, was used to obtain the resistivity of NaCl solutions of different concentration, ranging from 5×10^{-3} to 2.0 mol/L (Note: this also covered the anticipated range of resistivity values for the tailings slurry). These values were then used to evaluate the geometrical constant A/d for each electrode set, which were: 0.1623m for position E1, 0.1898m for positions E2 and E3, and 0.1857m for position E4. The lower constant recorded at electrode position 1 (E1) results from the presence of the non-conductive boundary at the base of the column. Without fringing effects, the theoretical value of the geometrical constant for this electrode arrangement is 0.125m. The relationship between ρ and R obtained during the calibration process is presented in Figure 3.

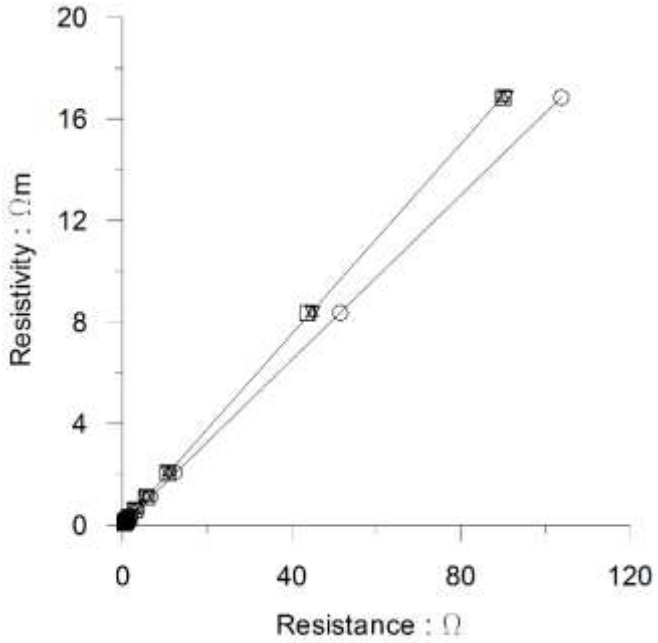

Figure 3. Relationship between electrolyte resistivity ρ and resistance R recorded during calibration of the sedimentation column and used to obtain the geometric constant A/d for each set of electrodes: E1 (○), E2 (□), E3 (Δ) and E4 (∇). Results for E2, E3 and E4 are virtually the same.

2.4 Test procedure

After initial sieving to remove material coarser than 0.3mm, the tailings were dried in an oven at 105°C and 2.3kg of dry material was mixed with sufficient deionised water to obtain a slurry with a solids content, P, of 55%. The solids content, also known as pulp density or concentration, is given by the mass of solids per kilogram of slurry. The mixture was placed inside a plastic container with an airtight lid and left to hydrate for four days.

Following hydration, the slurry was first placed in a rotary mixer for 30 minutes and then poured inside the sedimentation column. The 40mm gap left between the surface of the slurry and the top of the column allowed an airtight cap to be placed, which ensured no loss of slurry during initial agitation, as well as eliminating evaporative losses during the sedimentation stage. After vigorous agitation of the column to ensure a homogeneous mix, it was placed on a laboratory bench and initial readings of the height of the slurry, resistance at each electrode, and thermistor resistance taken.

Thereafter, values of the slurry-water interface height and electrode resistance were recorded; although no appreciable change in any of these quantities was observed after 4 to 5 hours, the test was conducted over a 24-hour period.

As only a limited mass of tailings was available for the study, following completion of the first test the material was dried at 105°C and reused in further tests. The same procedure was followed each time to monitor the sedimentation of slurries with solids contents of 50%, 52.5%. 55%, 57.5%, 60.5% and 65% (although tests were not performed in that order). Some of these solid contents are higher than values measured in the field, which range from 15% to 55% and are most commonly in the range of 40-55% (Vick 1990). However, it was noticed that when the solids content fell below 55% the slurry would settle below the third set of electrodes (E3 in Figure 2). Tests at higher solid contents allowed measurements to be recorded in three of the four electrode positions.

3 RESULTS

3.1 Sedimentation of slurry

Shortly after the start of a test it was possible to identify an interface between the slurry and the supernatant liquid. The vertical movement of this interface is presented in Figure 4, where settlement corresponds to the vertical movement of the interface relative to the original height of slurry at the start of a test. In all cases, settlement occurred quickly and the slurry reached a stable condition after only a few hours as noted above. Although the curves plotted in Figure 4 have been terminated shortly after settlement ceased, measurements were continued for 24 hours, which showed no further movement beyond what is shown. Total settlements and true vertical strains as a function of solids content are presented in Figure 5. Initial and final average porosities of the tailings mass, together with changes in porosity during sedimentation, are shown in Figure 6.

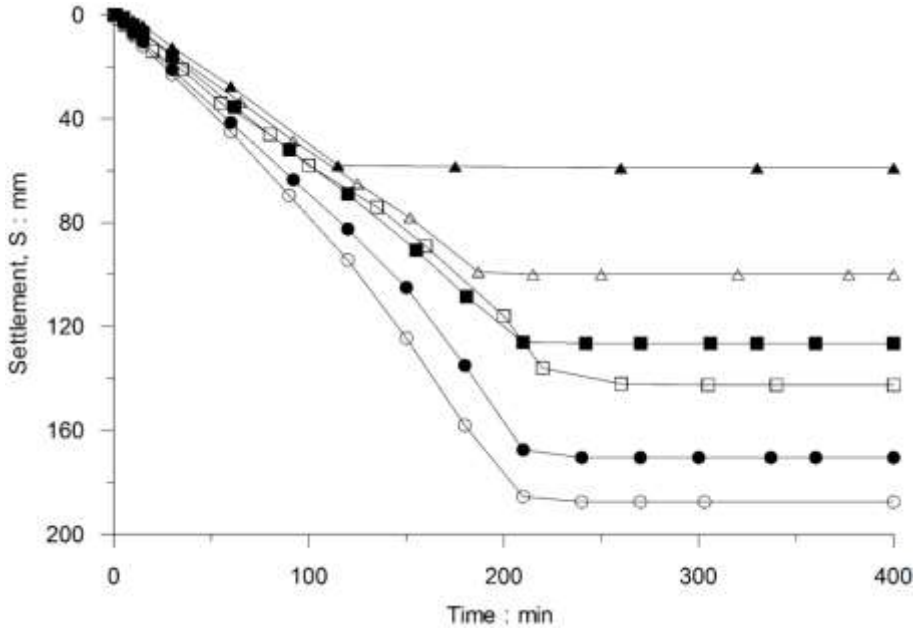

Figure 4. Vertical settlement plotted against time for different solids contents: 50% (○), 52.5% (●), 55% (□), 57.5% (■), 60.5% (Δ), and 65% (▲). Settlement refers to the vertical movement of the slurry-water interface with respect to the original position of the slurry surface at the start of a test.

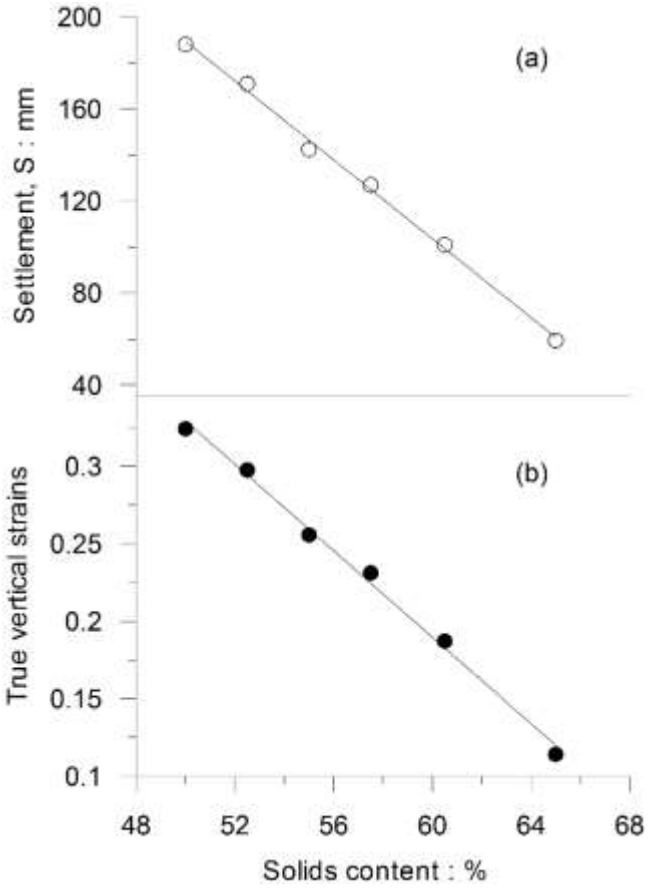

180

181 Figure 5. (a) Total settlement and (b) true vertical strains as a function of solids content.

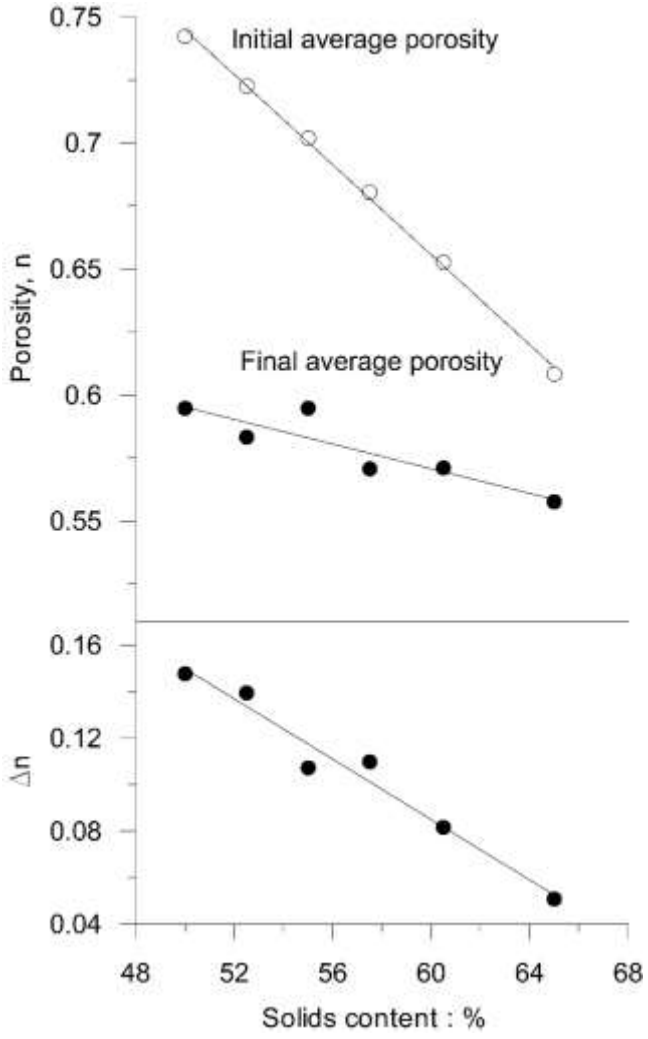

Figure 6. Initial and final average porosities for different solids content, together with changes in porosity during sedimentation.

3.2 Electrical measurements

The electrical resistivity of soil-water slurries containing low specific surface-area particles is affected primarily by electrolyte concentration and porosity (Santamarina et al 2001). In the work presented, where the tailings are non-plastic, it is possible to use empirical equations, such as the one proposed by Archie (1942), to relate the bulk resistivity of the mixture to the resistivity of the electrolyte (Klein and Santamarina 2003).

For saturated rock formations the Archie relationship can be written as

193 $$\frac{\rho_{mix}}{\rho_{el}} = a.n^{-m} \quad (2)$$

194 where ρ_{mix} is the bulk resistivity of the rock, ρ_{el} is the resistivity of the electrolyte filling the pore
195 space, *n* is the porosity of the rock . The exponent *m* is the *cementation exponent*, and is related to the
196 tortuosity and connectivity of the pore network within the rock and *a* is a correction factor, which is
197 valid over a particular range of porosities, *n*. A wide range of values have been reported for *m* and *a*
198 for different rock and sediment formations, with *a* typically in the range 0.4 – 2.5 and *m* = 1.2 – 2.5
199 (e.g. Worthington 1993; Santamarina et al 2001; Khalil and Santos 2011). Values of *a* and *m* are
200 characteristic for a given porous rock formation and are determined empirically. Archie (1942)
201 introduced a formation resistivity factor, *F*, representing the resistivity magnification related to the
202 electrolyte resulting from the presence of a non-conductive matrix (Schön 2004):

203 $$F = \frac{\rho_{mix}}{\rho_{el}} \quad (3)$$

204 Following equation (3) above, electrical resistivity measurements made in the sedimentation column,
205 corresponding to ρ_{mix}, were *normalised* by the resistivity of the pore-fluid ρ_{el} to derive values of the
206 resistivity formation factor, *F*. The resistivity of the pore-fluid was obtained by extracting supernatant
207 fluid at the end of a test and using the cell employed during the calibration stage. Figure 7 shows a
208 plot of pore-fluid resistivity against solids content. The numbers above the data points indicate the
209 order in which the tests were done.

210

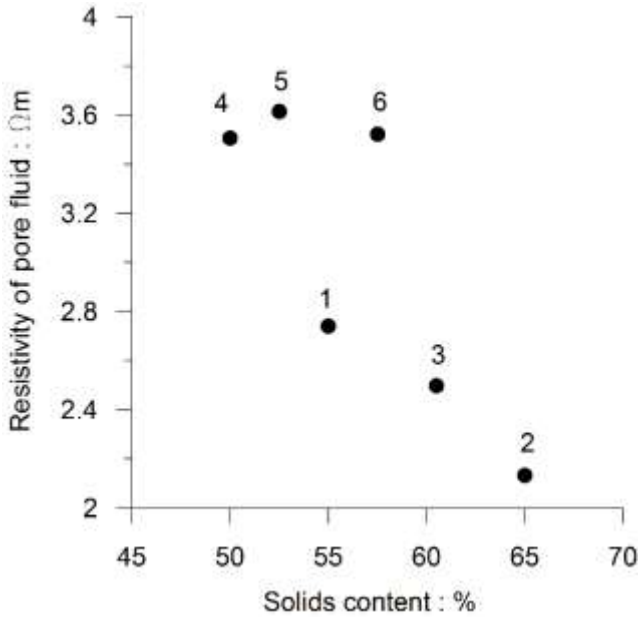

211

212 Figure 7. Variation in electrical resistivity of the pore fluid with solids content. Test number indicated
213 above symbols.

214

215 Variations in electrical resistivity with time, recorded at each electrode level within the sedimentation
216 column, are presented in Figure 8. Results are given in terms of Archie's formation resistivity factor
217 *F*. In addition, variations in *F* down the sedimentation column at the start and end of each test are
218 presented in Figures 9 and 10 respectively.

219 For slurries tested at solids contents of 50% and 52.5%, only measurements recorded at electrode
220 positions 1 and 2 (E1 and E2) are presented, as the final elevation of the slurry-water interface was at
221 the midpoint and just above plate electrode 3 (E3) respectively in these two tests. The equilibrium
222 position of the interface during the test performed at a solids content of 55% was 26mm above the top
223 of plate electrode 3 and the electrical field could have extended into the supernatant liquid. Hence the
224 final resistivity recorded at E3 in this test must be considered uncertain, especially since this is
225 significantly lower than values recorded at the other two electrode positions.

226 The final elevation of the slurry-water interface recorded in tests carried out at solids contents above
227 55% was sufficiently removed from the edge of plate electrode 3 (E3) to affect measurements. In

addition, in all except one test, this interface was below electrode 4, E4 (thus resulting in $F = 1$); at the highest solids content of 65% the plate electrodes at position 4 were only partially covered by the end of the test. No measurements were therefore recorded at electrode position 4 in any of the tests.

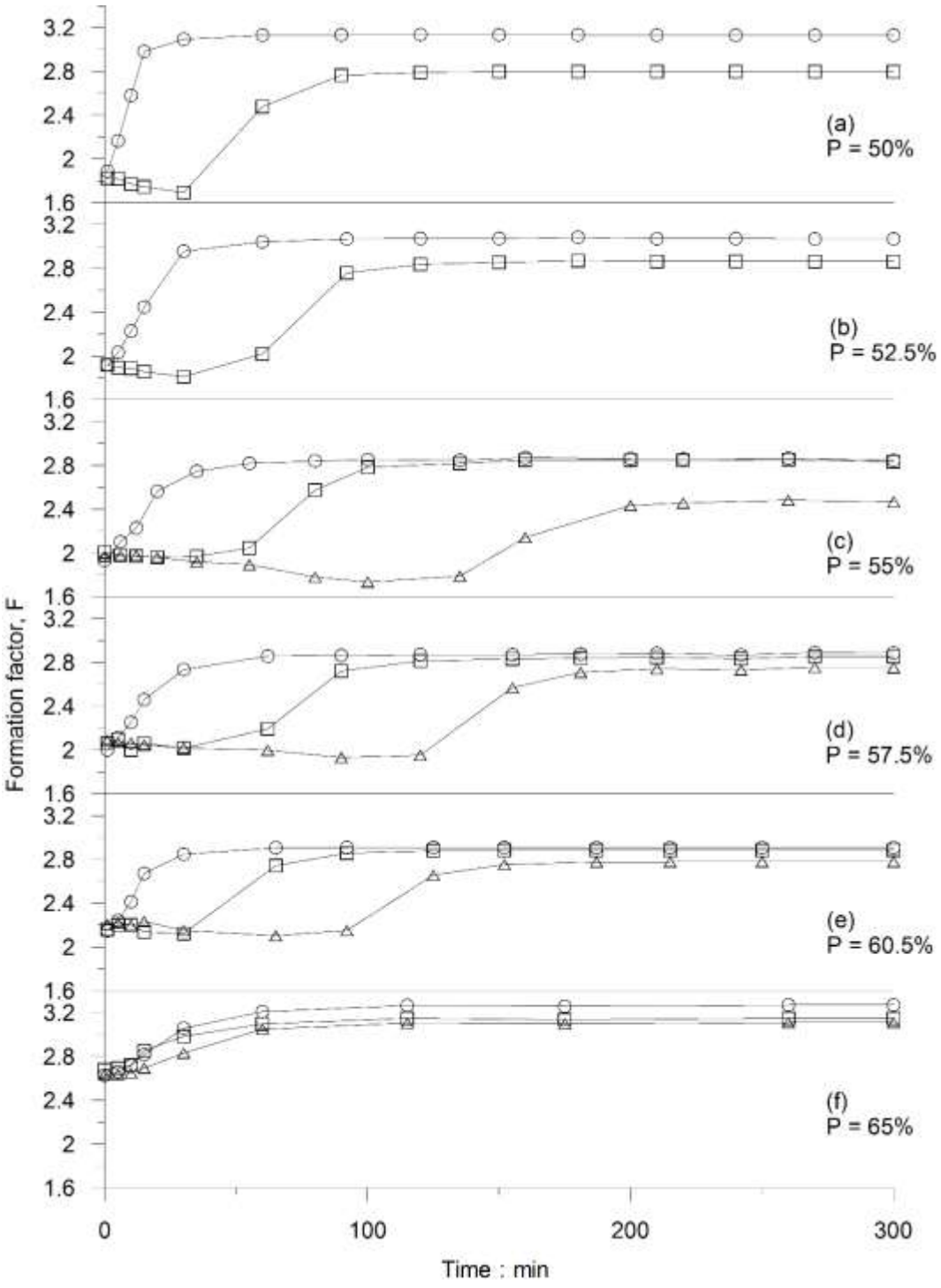

239

240 Figure 8. Variation in formation resistivity factor, *F*, with time recorded in tests performed at solids
241 contents of (a) 50%, (b) 52.5%, (c) 55%, (d) 57.5%, (e) 60.5% and (f) 65%. For times in excess of
242 300min the response remains constant. Electrode positions (see Figure 2): E1 (○), E2 (□), E3 (Δ). The
243 vertical scale is the same in all plots.

244

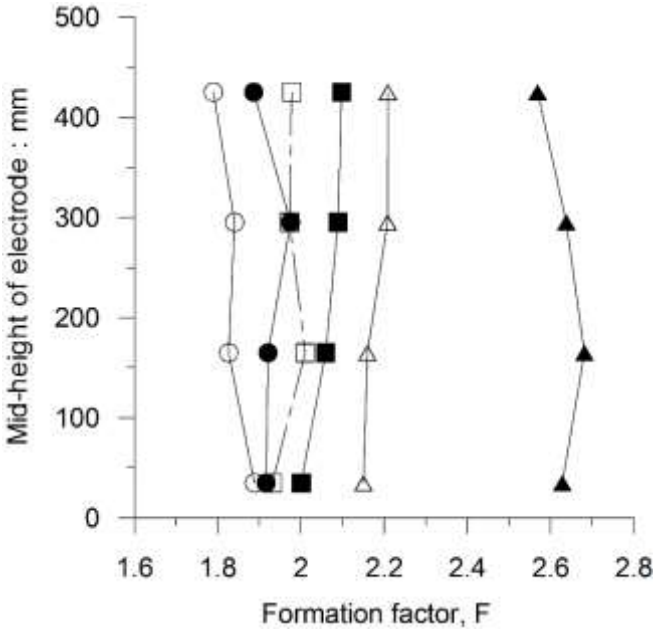

245

246 Figure 9. Formation resistivity factor, *F*, plotted against depth profiles at the start of a test for different

247 solids contents: 50% (○), 52.5% (●), 55% (□), 57.5% (■), 60.5% (Δ), and 65% (▲).

248

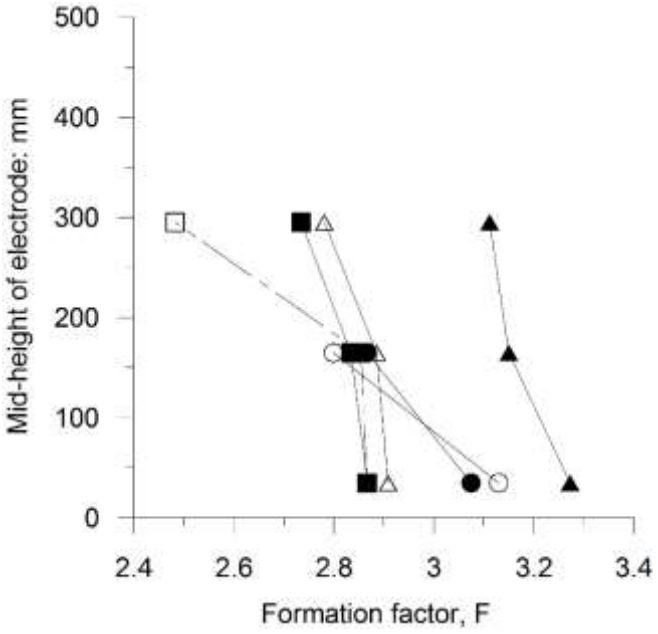

249

250 Figure 10. Formation resistivity factor, *F*, plotted against depth profiles at the end of a test (24-hours)

251 for different solids contents: 50% (○), 52.5% (●), 55% (□), 57.5% (■), 60.5% (Δ), and 65% (▲).

252

4 DISCUSSION

Results presented in Figure 4 to Figure 6 reveal how, for the range of solids contents under consideration, settlements, vertical strains, initial and final porosities, as well as changes in porosity during sedimentation, vary linearly with the mass of solids in the slurry. Figure 7, on the other hand shows no correlation between resistivity of the pore fluid and solids content. The same material was used for each test, and Figure 7 only indicates an increase in pore fluid resistivity with time. Whereas values are below 2.8Ωm in earlier tests (1 to 3), these increase to approximately 3.6Ωm in latter tests (4 to 6).

As the formation resistivity factor vary little with depth, this indicates homogeneous conditions at the start of each test (Figure 9). However, during subsequent sedimentation the response varied according to electrode position and solids content.

In all tests, the formation resistivity factor at electrode position 1 (E1) increases monotonically with time to a maximum value (Figure 8), which, according to equation (2) would be the result of a decrease in porosity *n*. At all other electrode positions and solid contents, except for the highest (65%), the formation factor initially decreases, as the coarser particles settle, and thereafter increases as material accumulates at a particular level. This trend, however, is less evident at higher solids contents, and the effect is not observed at a solids content of 65%.

A comparison of the times at which settlement of the slurry-water interface ceases and formation factor stabilises reveals that, in all cases, the latter precedes the former. This is expected, as no measurements were taken above the third set of electrodes. According to equation (2), a constant value of formation resistivity factor would imply no further change in porosity.

The plot of the variation in formation resistivity factor, *F*, with depth at the end of each test (Figure 10) shows that for solid contents ≥57.5% there is a well-defined pattern relating an increase in *F* with depth and solids content. For lower solids contents, although the formation factor increases with depth, the relationship with solids content does not hold. In particular, final values of formation factor measured at electrode position 1 (E1) are higher for solids contents of 50% and 52.5% than for

concentrations of 55% and above (with the exception of 65%). No explanation is advanced for this anomaly.

The variation in equilibrium bulk resistivity of the mixture with electrolyte resistivity has been plotted in Figure 11, which includes measurements recorded at each electrode level. The data has been modelled using Archie's law with a = 1 and m = 1.95 and is shown as a solid line. The plot reveals how pore-fluid resistivity controls bulk resistivity, as well as the effect of porosity and tortuosity on bulk resistivity.

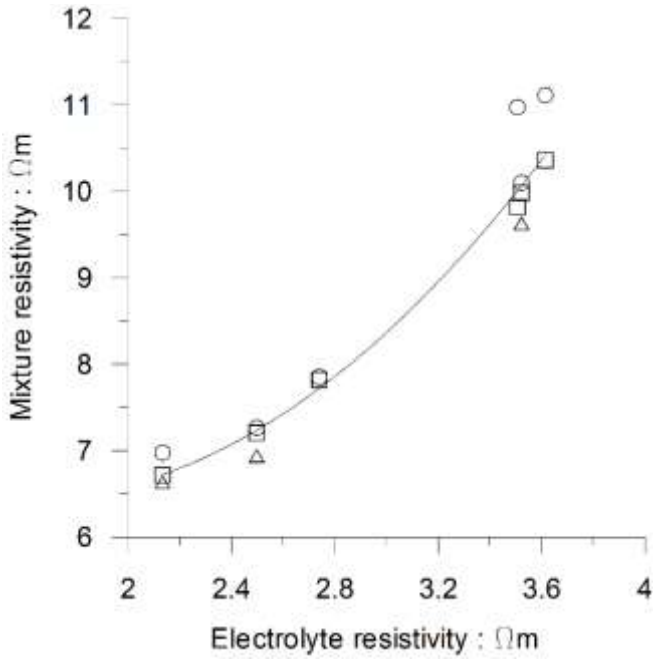

Figure 11. Equilibrium resistivity of the tailings mass as a function of pore fluid resistivity. Data modelled using Archie's law with a = 1 and m = 1.95 (solid line). Data points correspond to different electrode positions: E1 (○), E2 (□), E3 (Δ).

Formation resistivity factor as a function of porosity is presented in Figure 12, together with the trend obtained using Archie's law with a = 1 and m = 1.95 (shown as a solid line). The experimental data can be modelled using the empirical relationship presented in equation (2) with the two highlighted

295 points excluded from the fitting equation. The latter correspond to the formation factors obtained in
296 electrode position 1 (E1) for solid contents of 50% and 52.5%.

297

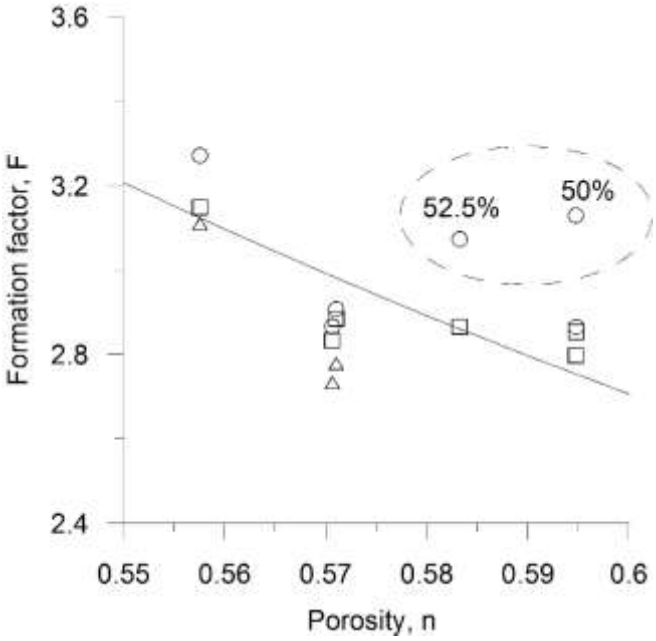

298

299 Figure 12. Formation resistivity factor as a function of porosity. Archie's law with a = 1 and m = 1.95
300 represented with a solid line. Data points correspond to different electrode positions: E1 (○), E2 (□),
301 E3 (Δ). Encircled data points correspond to measurements made at E1 on samples with indicated
302 solids content.

303

304 **5 CONCLUDING COMMENTS**

305 The main aim of this study was to assess the use of a simple experimental technique, previously
306 employed with clay slurries, to monitor the settling and sedimentation of mine tailings. A
307 sedimentation column, fitted with four electrode sets, was used to test slurries of solids contents over
308 the range 50%-65%. During sedimentation, temporal changes in electrical resistivity were recorded at
309 four electrode-set positions.

Test results showed a monotonic increase in resistivity with time at the base of the column; a maximum value was reached within one hour and, thereafter, resistivity remained constant. In all other electrode positions, an initial reduction in resistivity was followed by an overall increase to a constant final value. Constant resistivity is interpreted to correspond to a situation where there is no further change in the slurry porosity.

Bulk resistivity in particulate materials of low specific surface is controlled by the resistivity of the pore fluid and, therefore, results have been presented in terms of Archie's formation resistivity factor, *F*, corresponding to the ratio of bulk to pore fluid resistivity. This factor represents the increase in resistivity resulting from the presence of a non-conductive matrix in an electrolyte. Slurry resistivity at equilibrium was plotted as a function of pore fluid resistivity and the data modelled using Archie's law.

The test performed within the sedimentation column corresponds to what is usually known as an undrained settling test. In this test, which is used to assess the rate at which supernatant fluid separates from the slurry, as well as the minimum density obtained during subaqueous deposition, only the settlement of the slurry-water interface is recorded to produce a plot similar to that shown in Figure 4. The inclusion of electrodes allows a much better understanding of spatial variation in material properties.

For practical reasons, tests were performed within a relatively small sedimentation column and it is acknowledged that a larger column (e.g. Been and Sills, 1981) would not only accommodate a larger number of electrodes, but it would also increase the maximum stress experienced by the slurry at the base. A combination of tests performed in larger sedimentation columns and in oedometers, such as the hydraulic oedometer described in McCarter et al (2005), could be used to derive relationships between resistivity and void ratio. This, together with in-situ measurements of electrical resistivity, could be used to monitor the sedimentation and self-weight consolidation of tailings in the field (although the consolidation stage was not investigated in the current study).

NOTATION

A	electrode surface area (m^2)
a	correction factor
d	electrode separation (m)
F	formation resistivity factor
m	cementation exponent
n	porosity
R	bulk resistance (ohm)
ρ_{el}	resistivity of pore fluid (ohm-m)
ρ_{mix}	bulk resistivity of material (ohm-m)

ACKNOWLEGMENTS

RM would like to express his gratitude to Dr. Diaz for his encouragement and support; without his assistance this study would probably have never taken place.

REFERENCES

Azam, S. (2014a) Role of environmental geotechnics in mine tailings management. Environmental Geotechnics, 1(1): 68-69.

Azam, S. (2014b) Study on large strain consolidation of mine waste tailings. Environmental Geotechnics, 1(1): 48-55.

Archie, G. E. (1942) The electrical resistivity log as an aid in determining some reservoir characteristics. Trans. Am. Inst. Min. Metall. Engrs., 146(1): 54-62.

Been, K. and Sills, G. (1981) Self-weight consolidation of soft soils: an experimental and theoretical study. Geotechnique, 31(4): 519-535.

Blewett, J., McCarter, W.J, Chrisp, T.M, and Starrs, G. (2001) Monitoring sedimentation of a clay slurry. Goetchnique, 51(8): 723-728.

Blewett, J., McCarter, W.J., Chrisp, T.M, and Starrs, G. (2003) An experimental study on ionic migration through saturated kaolin. Engineering Geology, 70: 281-291.

Blight, G. (2010) Geotechnical engineering for mine waste storage facilities. CRC Press, The Netherlands, 634 pp.

EC (European Community) (2006). Directive 2006/21/EC of the European Parliament and of the Council of 15 March 2006 on the management of waste from extractive industries and amending Directive 2004/35/EC. Official Journal of the European Union L143/6.

Khalil, M.A. and Santos, F.A.M. (2011) Influence of degree of saturation in the electric resistivity – hydraulic conductivity relationship. In: Developments in Hydraulic Conductivity Research, Dr. O. Dikinya (ed), InTech, DOI: 10.5772/15667. Available from http://www.intechopen.com/books/developments-in-hydraulic-conductivity-research/influence-of-degree-of-saturation-in-the-electric-resistivity-hydraulic-conductivity-relationship [Accessed 05/01/2017].

Klein, K. A., and Santamarina, J. C. (2003) Electrical conductivity in soils: Underlying phenomena. Journal of Environmental & Engineering Geophysics, 8(4): 263-273.

Klein, K. A. and Santamarina, J.C. (2005) Soft sediments: wave-based characterization. International Journal of Geomechanics, 5(2): 147-157.

McCarter, W.J., Blewett, J., Chrisp, T.M, and Starrs, G. (2005) Electrical property measurement using a modified hydraulic oedometer. Canadian Geotechnical Journal, 42(2): 655-662.

Santamarina, J. C., Klein, K., and Fam, M. (2001) Soils and waves. John Wiley & Sons, Toronto, 488pp.

Schön, J. H. (2004) Physical properties of rocks: Fundamentals and principles of petrophysics (Vol. 18). In Handbook of Geophysical Exploration. Edited by K. Helbig and S. Treitel, Elsevier, New York.

Vick, S.G. (1990) Planning, design, and analysis of tailings dams. BiTech Publishers Ltd, Vancouver, 369 pp.

Wagner, N. and Scheuermann, A. (2017) Electromagnetic techniques in geoenvironmental engineering. Environmental Geotechnics, 4(1): 3-8.

Worthington, P.F. (1993) The uses and abuses of the Archie equations, 1: the formation factor – porosity relationship. J Appl Geophy, 30(3): 215-228.

Figure captions

Figure 1. Particle size distribution of the tailings sample after removal of particles retained in the 0.3mm sieve. Also shown, curves for coarse and fine gold and copper tailings from Blight (2010).

Figure 2. Sedimentation column showing location of electrodes (E1 to E4).

Figure 3. Relationship between electrolyte resistivity ρ and resistance R recorded during calibration of the sedimentation column and used to obtain the geometric constant A/d for each set of electrodes: E1 (○), E2 (□), E3 (Δ) and E4 (∇). Results for E2, E3 and E4 are virtually the same.

Figure 4. Vertical settlement plotted against time for different solids contents: 50% (○), 52.5% (●), 55% (□), 57.5% (■), 60.5% (Δ), and 65% (▲). Settlement refers to the vertical movement of the slurry-water interface with respect to the original position of the slurry surface at the start of a test.

Figure 5. (a) Total settlement and (b) true vertical strains as a function of solids content.

Figure 6. Initial and final average porosities for different solids content, together with changes in porosity during sedimentation.

Figure 7. Variation in electrical resistivity of the pore fluid with solids content. Test number indicated above symbols.

Figure 8. Variation in formation resistivity factor, F, with time recorded in tests performed at solids contents of (a) 50%, (b) 52.5%, (c) 55%, (d) 57.5%, (e) 60.5% and (f) 65%. For times in excess of 300min the response remains constant. Electrode positions (see Figure 2): E1 (○), E2 (□), E3 (Δ). The vertical scale is the same in all plots.

Figure 9. Formation resistivity factor, F, plotted against depth profiles at the start of a test for different solids contents: 50% (○), 52.5% (●), 55% (□), 57.5% (■), 60.5% (Δ), and 65% (▲).

Figure 10. Formation resistivity factor, F, plotted against depth profiles at the end of a test (24-hours) for different solids contents: 50% (○), 52.5% (●), 55% (□), 57.5% (■), 60.5% (Δ), and 65% (▲).

Figure 11. Equilibrium resistivity of the tailings mass as a function of pore fluid resistivity. Data modelled using Archie's law with a = 1 and m = 1.95 (solid line). Data points correspond to different electrode positions: E1 (○), E2 (□), E3 (Δ).

Figure 12. Formation resistivity factor as a function of porosity. Archie's law with a = 1 and m = 1.95 represented with a solid line. Data points correspond to different electrode positions: E1 (○), E2 (□), E3 (Δ). Encircled data points correspond to measurements made at E1 on samples with indicated solids content.